Multidimensional mixed quantum-classical description of the laser-induced desorption of molecules

C. Bach[1], T. Klüner[2], A. Groß[1]
[1] *Physik-Department T30, Technische Universität München, 85747 Garching, Germany*
[2] *Fritz-Haber-Institut, Faradayweg 4–6, 14195 Berlin, Germany*
(Dated: April 30, 2003)

A mixed quantum-classical method for the simulation of laser-induced desorption processes at surfaces has been implemented. In this method, the nuclear motion is described classically while the electrons are treated quantum mechanically. Still the feedback between nuclei and electrons is taken into account self-consistently. The computational efficiency of this method allows a multidimensional treatment of the desorption processes. We have applied this method to the laser-induced desorption of NO from NiO(100) using a potential energy surface that is based on *ab initio* calculations. By comparing our method to jumping wave-packet calculations on exactly the same potential energy surface we verify the validity of our method. We focus on the velocity, rotational and vibrational distributions of the desorbing NO molecules. Furthermore, we model the energy transfer to the substrate by a surface oscillator. Including recoil processes in the simulation has a decisive influence on the desorption dynamics, in particular as far as the rotational distribution is concerned.

PACS numbers: 82.20.Gk, 82.20.Wt

I. INTRODUCTION

The photon-stimulated and the electron-stimulated desorption of molecules from surfaces has been intensively studied in the last decades [1]. In both kind of processes, the desorption is induced by electronic transitions (DIET). In recent years, technological progress has made it possible to perform time-resolved laser pump-probe experiments in which the time evolution of DIET processes can be monitored in the femtosecond regime [2]. These experiments provide a wealth of information on the real-time dynamics of chemical processes at surfaces (see, e.g., Refs. [3, 4]).

Unfortunately, the experimental progress has not been accompanied by a corresponding development of theoretical tools for the realistic description of DIET processes. This is mainly due to the fact that the modeling of processes involving electronic transitions still represents a great challenge. First of all, the *ab initio* determination of excited state potentials is not possible using computational efficient density-functional theory schemes. One has to use quantum chemistry methods which are usually computationally very costly. And second, the simulation of the dynamics of DIET processes requires to treat both electronic and nuclear dynamics explicitly. There has been significant progress in the high-dimensional simulation of Born-Oppenheimer reaction dynamics at surfaces in recent years [5–7]. These studies in fact demonstrated the importance of the multidimensionality in the reaction dynamics. However, electronically non-adiabatic simulations of reactions at surfaces are usually limited to a few degrees of freedom [8]. This is caused by the difficulties in the theoretical treatment because of the different time scales in the electronic and nuclear motion.

In order to allow a multidimensional treatment of laser-induced desorption, we propose to use mixed quantum-classical schemes in which the nuclear motion is described classically while the electrons are treated quantum mechanically. Still the feedback between quantum and classical degrees of freedom has to be taken into account self-consistently. We have recently implemented such a scheme for the description of charge transfer processes in the scattering of molecules at surfaces [9, 10]. This mixed quantum-classical scheme is based on the fewest switches algorithm developed by Tully [11]. In this surface-hopping algorithm the number of state switches is minimized under the constraint of maintaining the correct statistical population of each state.

We have now extended this algorithm in order to address laser-induced reactions at surfaces. Combining ideas of previous treatments [11–14], we have in particular introduced an optical potential in order to simulate the collective influence of electronic excitations of the substrate. Our mixed quantum classical (MQC) methods allow the inclusion of the relevant nuclear coordinates of both adsorbates and substrate at sufficiently long propagation times to correctly describe thermalization and dissipation effects. In order to establish the validity of our scheme, we first compare the results of our methods to two-dimensional jumping wave-packet calculations [15] of the laser-induced desorption of NO from a NiO(100) using exactly the same potential energy surface that was derived from *ab initio* calculations [16].

This system has been well-studied experimentally [17, 18]. One of the most interesting experimental results is the bimodality that was observed in the velocity distribution of desorbing molecules [17]. Based on the wave-packet calculations it was proposed that the bimodality is a consequence of a bifurcation of the wave-packet due to the topology of the excited state potential energy surface [15].

In order to study the influence of additional degrees

of freedom on the desorption process, we extended the potential energy surface to in total seven dimensions by considering the remaining NO degrees of freedom and one surface oscillator coordinate. In the absence of any *ab initio* calculations we used a physically reasonable model potential for this extension. Indeed, the incorporation of the higher dimensionality, in particular the recoil effects at the surface turned out to strongly modify the desorption dynamics.

This paper is structured as follows. After this introduction we will first lay out our proposed mixed-quantum classical scheme for the description of laser-induced desorption processes at surfaces. Then we will address the construction of the high-dimensional potential energy surface. The results of our calculations will be discussed in detail, and then the paper ends with some concluding remarks.

II. THEORY

A. Model

DIET processes are usually described within the Menzel-Gomer-Redhead (MGR) model [19, 20] or the Antoniewicz model [21] which differ in the relative position of the minima in the ground and excited state potentials. Still, both models assume the same reaction steps which are illustrated in Fig. 1. First the system is excited by, e.g., a laser pulse. This pulse may directly excite the adsorbate, but most probably first the substrate becomes electronically excited with the creation of hot electrons (step 1). The adsorbate then becomes electronically excited in a Franck-Condon transition, for example by the transfer of one electron from the substrate (2). Such a mechanism has been proposed for the laser-induced desorption of NO from NiO [17], but also direct excitations have been suggested [22]. Since the minimum energy position of the ground and excited state in general differ, the adsorbate in the excited state becomes accelerated (3). After a certain period of time the adsorbate returns to the electronic ground state with the excess energy being transfered to the substrate (4). Depending on how much kinetic energy the adsorbate gains in this process, it might desorb (5) or not.

In fact the adsorbate might become electronically excited more than just once. This would correspond to a DIMET process: desorption induced by multiple electronic excitations. As far as NO/NiO is concerned, however, the linear dependence of the desorption yield on the laser fluency [23] leads to the exclusion of multiple excitations.

One of the problems encountered when modeling such processes is the huge number of electronic substrate states involved which have to be treated quantum mechanically. It is clear that it is neither feasible nor necessary to explicitly include all these substrate states into our simulation. The reaction dynamics is dominated by

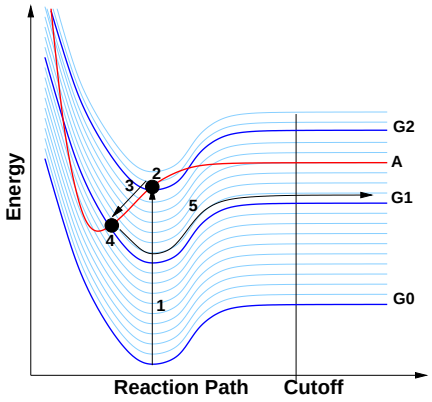

FIG. 1: Schematic drawing of a DIET process. The potential curves labeled G0–G2 correspond to the adsorbate ground state with different substrate excitations, while the curve labeled A corresponds to an excitation of the adsorbate. Thin dashed lines represent the adsorbate ground state together with the not explicitly involved substrate states. The numbers 1–5 indicate the five steps of the desorption process.

a few adsorbate states, which have to be taken into account. But the main effect of the substrate states of coupling different adsorbate states either to each other or to an external electromagnetic field can be treated collectively. To model this effect we combine ideas from Tully's fewest switching algorithm [11] and generalized surface hopping method [12] with those of Brenig [13] and Saalfrank [14] who introduced optical potentials in the description of DIET processes. First we separate the nuclear from the electronic degrees of freedom, i.e. the Hamilton operator H is split into the kinetic energy T_R of the nuclear coordinates R and an electronic part H_e depending explicitly on the electronic coordinates r and parametrically on the position of the nuclei R.

$$H(r,R) = T_R + H_e(r,R) \tag{1}$$

The electronic wave function Φ is expanded into the explicitly treated excited adsorbate states ϕ_i and a collective state ψ containing the molecular ground state together with the continuum of substrate excitations.

$$\Phi(r,R,t) = \sum_i c_i(t)\phi_i(r,R) + \psi(r,R,t)$$

The influence of the collective state ψ can be taken into account by an effective non-Hermitian Hamiltonian (see chapter 16 in [24])

$$H_{eff}(r,R) = T_e + V_{eff}(r,R) + i\Delta(r,R) \tag{2}$$

where T_e is the kinetic energy operator for the electrons. The effective potential V_{eff} and the optical potential Δ are real functions of r and R. In a Newns-Andersson picture Δ is related to the lifetime broadening of a resonance state which can be determined via [25]

$$\Delta(E) \;=\; \pi \sum_{\mathbf{k}} |V_{\mathbf{k}}|^2 \delta(E - \varepsilon_{\mathbf{k}}) \tag{3}$$

With the effective Hamiltonian and a diabatic (i.e. $\nabla_R \phi_i = 0$) representation of the wave functions ϕ_i the electronic Schrödinger equation has the following form

$$\dot{c}_j = -\frac{i}{\hbar}\sum_i c_i V_{ji} + \frac{1}{\hbar}\sum_i c_i \Delta_{ji}, \tag{4}$$

where the matrix elements V_{ij} and Δ_{ji} are defined as

$$\begin{aligned} V_{ji} &\equiv \langle\phi_j|T_e + V_{eff}(r,R)|\phi_i\rangle \\ \Delta_{ji} &\equiv \langle\phi_j|\Delta(r,R)|\phi_i\rangle \ , \end{aligned} \tag{5}$$

respectively. For the diagonal elements of the density matrix $a_{ji} \equiv c_j^\star c_i$ this leads to

$$\dot{a}_{jj} = \sum_i b_{ji} + \sum_i \frac{2}{\hbar}\Re\left[a_{ji}\Delta_{ji}\right], \tag{6}$$

with $b_{ji} \equiv \frac{2}{\hbar}\Im\left[a_{ji}V_{ji}\right]$. Note that for a normalized wave function Φ the occupation probability a_{cc} for the "rest" is simply given by $a_{cc} \equiv 1 - \sum_j a_{jj}$ leading to

$$\dot{a}_{cc} = -\sum_j \dot{a}_{jj} = -\frac{2}{\hbar}\sum_{ij}\Re\left[a_{ji}\Delta_{ji}\right], \tag{7}$$

since $\sum_{ji} b_{ji} = 0$. The nuclear coordinates R are treated classically and obey the Newtonian equation of motion

$$\ddot{R} = \frac{-1}{M}\nabla\left[\frac{\langle\psi_{occ}|H_e|\psi_{occ}\rangle}{\langle\psi_{occ}|\psi_{occ}\rangle}\right], \tag{8}$$

where ψ_{occ} is the currently occupied state. Using classical equations of motion for the nuclei is a reasonable approximation as long as hydrogen is not involved.

These equations are equivalent to the ones that have been derived in the generalized surface hopping method [12]. In our scenario, however, upon a transition to the continuum state we assume that the whole excess energy is taken up by the substrate electrons, as it is usually done in the modeling of laser-induced desorption [8]. This means that upon a switch to the continuum state we just make a Franck-Condon transition, i.e. we transfer the molecule to the ground state potential with its kinetic energy preserved and perform ordinary Born-Oppenheimer molecular dynamics until the final fate of the molecule has been determined.

If just one electronically excited state is considered, then the equations become much simpler. According to Eqs. 6 and 7, the de-excitation rate is directly given by

$$\dot{a}_{11} \ = \ -\dot{a}_{cc} \ = \ \dot{c}_1 c_1^* + c_1 \dot{c}_1^* = \frac{2a_{11}\Delta}{\hbar}. \tag{9}$$

In fact, for such a situation no electronic Schrödinger equation has to be integrated.

Our method could in principle also be extended in order to include the excitation process. Furthermore, taking explicit time dependence into account is also straightforward. This could be used, e.g., to model the pulse shape of the exciting laser or the thermalization of hot electrons in the case of an indirect process.

B. Procedure

We start our trajectories in the excited state where they move classically for a certain time. After a Franck-Condon transition the movement of the molecule is continued on the ground state potential for a maximal propagation time or until it reaches a certain distance Z_{Cutoff} from the surface and is considered desorbed.

The trajectories are started around the position of the ground state minimum assuming a Gaussian distribution in position and momentum according to the curvature of the ground state potential energy surface. This corresponds to a harmonic approximation for the potential at the minimum position. In principle the distributions should be given by the true ground state wave function, but since the masses of the nuclei are rather large and the anharmonicity of the potential is small, this is a good approximation.

After each integration step in the excited state we decide, according to the decay probability $p = \frac{2\Delta(R)dt}{\hbar}$, whether to continue in the excited or the ground state.

For constant Δ this procedure is equivalent to the Gadzuk scheme [26]) as used in [17]. In this scheme the residence times are kept fixed and the overall result is obtained by averaging over the different residence times with weight function $w_\tau(t) = \frac{1}{\tau}\exp(-t/\tau)$, where the average residence time or resonance lifetime τ is an adjustable parameter directly connected to the strength of the optical potential

$$\tau = \frac{\hbar}{2\Delta}. \tag{10}$$

C. Potentials

The potential energy surfaces we used in our simulation are based on two two-dimensional potentials V_{ai} from Klüner et al. [27] one is representing the electronic ground state and the other a charge transfer state where an electron from the substrate is transfered into an adsorbate state. These potentials were obtained by fitting analytical expressions to energies from ab initio calculations. The two degrees of freedom used are the molecule surface distance Z and the polar angle θ.

In order to come to a complete description of the NO molecule we extended the *ab initio* two dimensional potentials to six dimensions. In the absence of any *ab initio* results we were required to use a model potential for the additional degrees of freedom. Thus the particular choice of the parameters has to be considered as an educated guess. We like to point out, however, that the qualitative results we obtained did not depend very sensitively on the particular choice of parameters.

$$\begin{aligned} V^s_{6D}(X,Y,Z,r,\theta,\phi) = V^s_{ai}(Z,\theta) + V_{cor}(X,Y,Z) \\ +V_{az}(X,Y,Z,\phi) + V^s_{NO}(r) \end{aligned} \tag{11}$$

The upper index s is either g or e, denoting the ground or the excited state. For potentials where this index is absent we do not distinguish between the two states. The X and Y coordinate give the lateral position on the surface, ϕ is the azimuthal angle and r is the N–O distance in the NO molecule. The corrugation potential V_{cor} is given by

$$V_{cor}(X,Y,Z) = \frac{C_{cor}}{4} e^{-\lambda_{cor}(Z-Z_0)} \left(2 - \cos(G_X X) - \cos(G_Y Y)\right), \quad (12)$$

and the azimuthal dependence is

$$V_{az}(X,Y,Z,\theta,\phi) = \frac{C_{az}}{2} e^{-\lambda_{az}(Z-Z_0)} \cos(2\phi)\sin(\theta)\left(\cos(G_X X) - \cos(G_Y Y)\right). \quad (13)$$

This corresponds to a molecule with two equal atoms, but as an first approximation it will suffice. The strength of the corrugation was set to $C_{cor} = 1.0$ eV and for the azimuthal dependence $C_{az} = 0.25$ eV with decay length of $\lambda_{cor} = \lambda_{az} = \frac{1}{2}$ Å^{-1}. The lattice constants G_X and G_Y are set to the Ni–Ni distance of the NiO(100) surface $G_X = G_Y = 2.942$ Å as used in [27]. The NO-potential is given by a Morse-Potential with different parameters for the ground and the excited state.

$$V^s_{NO}(r) = C^s_{NO}\left(1 - e^{-\alpha_s(r-r_s)}\right)^2 \quad (14)$$

The parameters used for the N-O potential were $C^g_{NO} = 6.5$ eV, $\alpha_g = 1.68$ Å$_{-1}$ and $r_g = 2.175$ a$_0$ in the ground state and $C^e_{NO} = 4.5$ eV, $\alpha_g = 1.50$ Å$_{-1}$ and $r_g = 2.225$ a$_0$ in the excited state in accordance with [28].

In order to model recoil effects of the substrate we included a surface oscillator with coordinate s by directly coupling a harmonic potential to the desorption coordinate which in our case is the distance from the surface Z

$$V^s_{\mathrm{N}+osc}(s,Z,R) = V^s_{\mathrm{N}}(Z-s,R) + V_{osc}(s) \quad (15)$$

where R denotes all other coordinates. The mass of the oscillator is taken equal to the mass of a Ni atom (58 amu) since NO is adsorbed on top of a Ni atom. The oscillator frequency has been chosen to correspond to the average value of a Debye spectrum, as it is usually done in simulations using the surface oscillator model [29]. The Debye temperature of NiO has been estimated to be between 500 and 600 K [30]. Accordingly, we have set the oscillator frequency to $\hbar\omega = 27$ meV. Anyway, the effect of the surface oscillator on the desorption dynamics is not very sensitive to the particular choice of the frequency. In the following we will report results of 2D and 6D simulations without and with the surface oscillator, denoted by 2D, 3D, 6D, or 7D calculations, respectively.

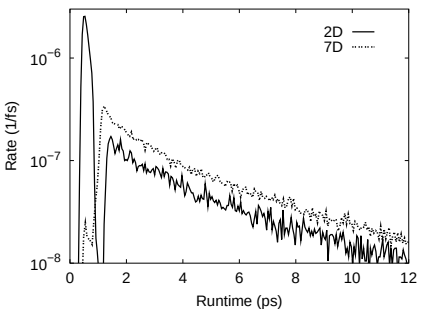

FIG. 2: Desorption rate as a function of time (excitation at time $t = 0$) in the two-dimensional (solid line) and the seven-dimensional simulations (dash-dotted line). The 2D results have been obtained with a cutoff distance of $Z_{Cutoff} = 12.5$ a.u. while in the 7D calculations $Z_{Cutoff} = 16.0$ a.u. has been chosen.

III. RESULTS AND DISCUSSION

In order to validate the classical treatment of the nuclear coordinates we first tried to reproduce the wave packet results from Klüner et al. [15] by performing equivalent two dimensional molecular dynamics simulations using the same ab initio potential energy surface and the Gadzuk-Scheme with a resonance lifetime of 24.19 fs (= 1000 au). For that lifetime the wave packet calculations gave a desorption yield of 3.3% whereas the classical simulations lead to 4.8%. This was puzzling as we expected the wave packet results to give a higher yield due to desorption from classically forbidden tails of the wave function. Closer examination of the desorption probability as a function of time helped to resolve this discrepancy. As can be seen in figure 2 there are two kinds of desorbing trajectories, early (within the first 1.2 picoseconds) and late ones. The wave packet results were obtained by propagating in the ground state until the desorption yield saturated after 1.2 ps. Note that for the 2D results there is a gap in the desorption probability at that time. When we consider only the early desorbing trajectories the desorption probability goes down to 2.91% in much better agreement with the wave packet results. For better comparison with the wave packet simulations a cutoff distance of 12.5 a$_0$ was chosen. When going to larger cutoff distances naturally the early desorption probability goes down (2.49% for 16.0a_0 and 1.56% for 20.0 a$_0$) and also the gap in the desorption flux vanishes. The total desorption probability does not depend on the cutoff distances. When not comparing to the wave packet results we will use a cutoff distance of 16.0 a$_0$ since at 12.5 a$_0$ the binding energy is still 10 meV. Note that for our method the computational cost in increasing the cutoff distance are small compared to those in the wave packet case.

The phenomenon of the early and late desorbing molecules can be understood by closer examination of single trajectories and by taking the position of the

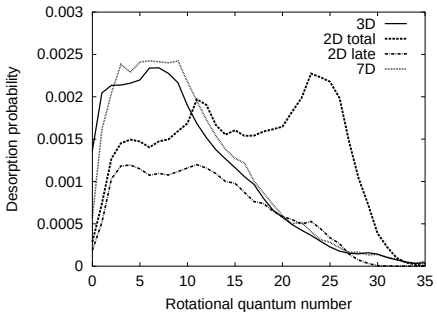

FIG. 3: Comparison of the rotational momentum distributions with and without the surface oscillator.

potential energy surface minima into account. In the ground state minimum the NO molecule is tilted from the surface normal by 45 degrees. The excited state the minimum is an upright position closer to the surface. Thus upon excitation the molecule is accelerated towards the surface and into an upright position. At the life times we used most molecules relax to the ground state before they reach the excited state minimum. On the ground state the molecules hit the repulsive potential wall and either scatter directly into the vacuum, giving the early desorbing species, or start to rotate in front of the surface and are trapped or desorb after one or more rotations, leading to the late species. The molecules scattered directly into the vacuum have high translational and rotational momentum. The difference in the rotational momentum distribution between the late and the early trajectories can be seen in fig. 3 where we plotted the distributions for all and the late trajectories only. The late molecules show a broad peak between $J = 3$ and 11 and fall off for higher momenta. The early species shows a large peak at $J = 25$ and a smaller one at $J = 12$. Note that for a free rotating NO molecule the rotational period T is connected to the rotational quantum number J via $T = \frac{2\pi\theta}{\hbar}\frac{1}{J}$, where $\frac{2\pi\theta}{\hbar}$ is equal to 9.79 ps. Thermalization would eventually lead to the suppression of the late desorption but on a much larger timescale of several picoseconds (the total time scale of our simulation is only twelve picoseconds).

There is good qualitative agreement between the velocity distributions of the early desorbing classical trajectories and the wave packet results from Ref.[15]. However, when also considering the late trajectories the shape of the momentum distributions changes considerably and only for the highest rotational states the agreement remains. We also compared the Gadzuk-Scheme for relaxation into the ground state with decay using a either constant or exponentially decreasing optical potential. The mean lifetime τ and the strength of the optical potential Δ_0 are related via

$$\Delta_0 = \frac{\hbar}{2\tau} \tag{16}$$

and the spatial dependence of optical potential is given

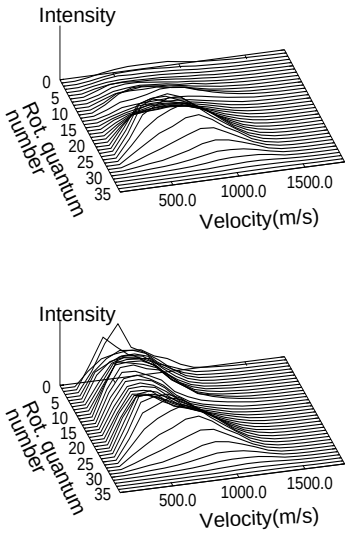

FIG. 4: Complete momentum distributions for early (top) and all (bottom) desorbing molecules in the two-dimensional MQC simulation.

by

$$V_{opt} = V_{opt}(Z) = \Delta_0 e^{-\gamma(Z-Z_0)} \tag{17}$$

Z_0 is the ground state equilibrium distance of the NO molecule from the surface. A zero inverse decay length γ corresponds to a constant V_{opt}. Using an exponentially decaying optical potential is motivated by the fact that the coupling between the ground and the charge transfer state is given by the overlap of the molecular state with the bulk electrons. As expected we found no significant difference between the constant optical potential and the Gadzuk-Scheme, neither for the desorption probability nor the momentum distributions. More surprising was that switching on the exponential decrease of the optical potential had basically no effect on the momentum distributions and only changed the total desorption probability.

When first extending the two dimensional *ab initio* potential to six dimensions we used the gas phase value of $r_{NO} = 2.377\mathrm{a}_0$ for the NO^- ion equilibrium distance. As is long known [1] and can be seen in figure 5 (thin solid line) this is leading to unrealistic high vibrational excitations. However when using a separation of $0.05\mathrm{a}_0$, as suggested in [28] between the atomic and ionic equilibrium distance, we get good agreement with the experimental values.

Another observation from varying the NO^- equilibrium distance is, that the total desorption probability did not change within the level of the accuracy of our simulations. This indicates that energy transfer from the vibrational coordinate into other degrees of freedom is very low, since when using the gas phase value for the N–O distance half of the trajectories have enough energy

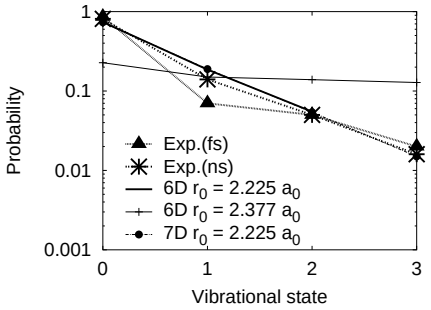

FIG. 5: The vibrational excitation for different models. The experimental values are taken from [18].

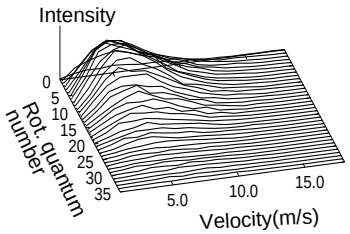

FIG. 6: Complete momentum distribution for the 7D simulation.

to overcome the desorption barrier, but only 4.97 percent actually desorb within reasonable time. Not only the desorption probability hardly changes with r_{NO^-} also the momentum and rotational momentum distributions do not vary.

Since the mass of the substrate atoms and the NO molecule is comparable, recoil processes during the desorption process are probable. In order to include energy transfer to the substrate in the simulations, we have coupled the 2D and 6D potentials to a surface oscillator with realistic parameters, as described in the previous section. The computational costs of this extension are rather small.

In Tab. I we have collected the main results with respect to the desorption probability and the rotational temperature of desorbing molecules according to the 2D, 3D, 6D and 7D calculations. Going from 2D to 6D, i.e., including the remaining molecular degrees of freedom in the simulations, has only a small influence on the desorption dynamics. The same is also true for the transition from 3D to 7D.

However, taking recoil processes of the substrate into account by including a surface oscillator changes the outcome of the trajectory calculations significantly. While the total desorption probability is only reduced by about 1%, the effect on the early desorption channel is really dramatic: it is reduced by a factor of eight. This can also be seen in the desorption rate in Fig. 2, where the initial "early" peak is basically absent in the 7D results. This also affects the rotational momentum distribution. While in the 2D calculations we obtain a double peaked structure with a large probability for high rotational quantum numbers j, the inclusion of the surface oscillator causes the suppression of the peak at high j. The distribution is similar to that of the late molecules in the rigid surface case. This results in greatly reduced mean rotational energy in desorption, 366 K and 395 K for 3D and 7D calculations, respectively, instead of 770 K and 883 K for 2D and 6D calculations, respectively. These reduced rotational temperatures are in fact in much better agreement with experiment [17].

	2D	3D	6D	7D
z_{CO} (a_0)	12.5	16.0	16.0	16.0
P_{des} (%)	4.84	3.63	4.74	4.02
P_{early} (%)	2.93	0.32	2.53	0.32
E_{rot} (K)	770	366	883	395

TABLE I: Desorption probabilities and mean rotational energies according to the 2D, 3D, 6D and 7D calculations. Early means desorption within the first 1.2 picoseconds.

As far as the comparison between experiment and theory with respect to the velocity distribution is concerned, however, the agreement is greatly reduced if the late desorption channel and the surface oscillator are taken into account. In Fig. 6, we have plotted the momentum distribution according to the 7D calculations. The momentum distribution for the 3D simulation is rather similar whereas the 6D results compare well to the 2D distribution as shown in fig. 4. There is no indication of any bimodal velocity distribution which was found in the experiment [17] and which was also reproduced in the wave-packet calculations [15]. Note that apart from an overall scaling due to the reduced desorption probability the shapes of the velocity distributions summed over all rotational momenta are almost identical for all dimensionalities used.

These findings do not necessarily imply that the conclusions of Ref. [15] with respect to the origins of the bimodality in the velocity distribution are no longer valid. In Ref. [15] it was proposed that the bimodality is a consequence of a bifurcation of the wave-packet due to the topology of the excited state potential energy surface. It might well be that this explanation is still correct. However, in the simulations only one excited charge transfer state potential out of a great number of charge transfer states [27] has been chosen. Possibly more than one excited state might be involved in the desorption process. Furthermore, the extension of the two-dimensional *ab initio* potential to seven dimensions using a physically reasonable model potential could not be realistic enough. This will be checked by mapping out higher-dimensional potential energy surfaces through quantum chemical calculations. Finally, the consideration of a more complex spatially varying transition probability could lead to a better agreement between theory and experiment. If the

de-excitation mainly occurs at specific configurations of the adsorbate, this can have a strong effect on the desorption dynamics. From a computational point of view, the simulation of such processes within our mixed quantum-classical scheme is indeed feasible and will be addressed in the future.

IV. CONCLUSION

In this paper we have presented a mixed-quantum classical scheme for the description of laser-induced desorption processes in which the nuclear motion is treated classically while the electron dynamics is treated quantum mechanically. The main motivation for such a scheme is its computational efficiency which allows a realistic high-dimensional treatment of the desorption dynamics. We first showed that our method is able to reproduce the results of lower-dimensional jumping wave-packet calculations for the desorption on NO from NiO(100). This confirms that quantum effects are indeed negligible in the nuclear dynamics of molecules such as NO.

Furthermore, we have demonstrated that our method is suited for a high-dimensional treatment on a long time-scale. We have simulated the laser-induced desorption using a seven-dimensional potential energy surface including all NO degrees of freedom and one surface oscillator coordinates. We find that the laser-induced desorption dynamics of NO/NiO(100) is rather complex requiring long simulation times. The inclusion of the surface oscillator has a dramatic effect on the desorption dynamics, in particular on the rotational state distribution. In our high-dimensional treatment we are not able to reproduce the bimodality found in the experiment. We speculate that this might due to the fact that we only included one excited-state potential in the simulations or that the extension of the potential energy surface to seven dimensions using a model potential is not realistic enough. Alternatively, a realistic, spatially varying transition probability could improve the agreement with the experiment. Future research along this line is in progress.

[1] F. M. Zimmermann and W. Ho, Surf. Sci. Rep. **22**, 127 (1995).
[2] M. Bonn, A. W. Kleyn, and G. J. Kroes, Surf. Sci. **500**, 475 (2002).
[3] M. Bonn, S. Funk, C. Hess, D. N. Denzler, C. Stampfl, M. Scheffler, M. Wolf, and G. Ertl, Science **285**, 1042 (1999).
[4] H. Petek, M. J. Weida, H. Nagano, and S. Ogawa, Science **288**, 1402 (2000).
[5] A. Groß, Surf. Sci. Rep. **32**, 291 (1998).
[6] G.-J. Kroes, Prog. Surf. Sci. **60**, 1 (1999).
[7] A. Groß, Surf. Sci. **500**, 347 (2002).
[8] H. Guo, P. Saalfrank, and T. Seidman, Prog. Surf. Sci. **62**, 239 (1999).
[9] C. Bach and A. Groß, Faraday Diss. **117**, 99 (2000).
[10] C. Bach and A. Groß, J. Chem. Phys. **114**, 6396 (2001).
[11] J. C. Tully, J. Chem. Phys. **93**, 1061 (1990).
[12] D. S. Sholl and J. C. Tully, J. Chem. Phys. **109**, 7702 (1998).
[13] W. Brenig, Z. Phys. B **23**, 361 (1976).
[14] P. Saalfrank, Chem. Phys. **193**, 119 (1995).
[15] T. Klüner, H.-J. Freund, V. Staemmler, and R. Kosloff, Phys. Rev. Lett. **80**, 5208 (1998).
[16] T. Klüner, H.-J. Freund, J. Freitag, and V. Staemmler, J. Mol. Catal. A **119**, 155 (1997).
[17] T. Mull, B. Baumeister, M. Menges, H.-J. Freund, D.Weide, C. Fischer, and P. Andersen, J. Chem. Phys. **96**, 7108 (1992).
[18] G. Eichhorn, M. Richter, K. Al-Shamery, and H. Zacharias, Surf. Sci. **368**, 67 (1996).
[19] D. Menzel and R. Gomer, J. Chem. Phys. **41**, 3311 (1964).
[20] P. A. Redhead, Can. J. Phys. **42**, 886 (1964).
[21] P. R. Antoniewicz, Phys. Rev. B **21**, 3811 (1980).
[22] H. Zacharias, G. Eichhorn, R. Schliesing, and K. Al-Shamery, Appl. Phys. B **68**, 605 (1999).
[23] G. Eichhorn, M. Richter, K. Al-Shamery, and H. Zacharias, J. Chem. Phys. **111**, 386 (1999).
[24] R. G. Newton, *Scattering Theory of Waves and Particles* (McGraw-Hill, 1966).
[25] R. Brako and D. M. Newns, Rep. Prog. Phys. **52**, 655 (1989).
[26] J. W. Gadzuk, Surf. Sci. **342**, 345 (1995).
[27] T. Klüner, H.-J. Freund, J. Freitag, and V. Staemmler, J. Chem. Phys. **104**, 10030 (1996).
[28] T. Klüner, S. Thiel, H.-J. Freund, and V. Staemmler, Chem. Phys. Lett. **294**, 413 (1998).
[29] A. Groß and W. Brenig, Surf. Sci. **302**, 403 (1994).
[30] K. S. Upadhyaya, G. K. Upadhyaya, and A. N. Pandey, J. Phys. Chem. Solids **63**, 127 (2002).